

First-principles study of superconductivity in high-pressure boron

D. A. Papaconstantopoulos* and M. J. Mehl†

Center for Computational Materials Science, Naval Research Laboratory, Washington, D.C. 20375-5345

(Received 20 November 2001; published 7 May 2002)

We study superconductivity in boron using first-principles LAPW calculations, the rigid-muffin-tin approximation, and the McMillan theory. Our results point to an electron-phonon mechanism producing transition temperatures near 10 K at high pressures, in agreement with recent measurements.

DOI: 10.1103/PhysRevB.65.172510

PACS number(s): 74.70.-b, 71.20.Dg

I. INTRODUCTION

In a recent paper, Eremets *et al.*¹ reported experiments where boron transforms from a nonmetal at normal pressures to a superconductor at very high pressures above 160 GPa. They presented results that showed an increase of the superconducting temperature T_c from 6 K at 175 GPa to 11 K at 250 GPa.

Previous theoretical studies on the metallization of boron based on first-principles total-energy calculations² predicted that the 12-atom insulating form of boron (α_{12} B) at atmospheric pressure transformed to a metallic body-centered tetragonal phase at 210 GPa and subsequently to an fcc structure at 360 GPa.

In this work we performed total-energy and band-structure calculations for the rhombohedral α_{12} B and fcc phases. Our results for the fcc phase were used as an input to the rigid-muffin-tin (RMT) theory of Gaspari and Gyorffy³ to determine the value of the Hopfield parameter η and subsequently evaluate the coupling constant λ and T_c . Our results for the parameter η give values comparable to those reported in the past⁴ for metallic hydrogen at very high pressure. Assuming that the fcc phase is the real high-pressure structure in the experiments of Eremets *et al.*,¹ this indicates that the simple RMT theory accounts for high-pressure superconductivity in boron.

II. THEORY AND RESULTS

In this work we have applied the RMT theory³ to calculate the Hopfield parameter η given by the expression

$$\eta = \frac{E_F}{\pi^2 N(E_F)} \sum_l 2(l+1) \sin^2(\delta_{l+1} - \delta_l) \frac{N_l N_{l+1}}{N_l^{(1)} N_{l+1}^{(1)}}, \quad (1)$$

where δ_l is the scattering phase shift at the Fermi energy E_F and angular momentum l , $N_l^{(1)}$ is the single-scatterer density of states, which, as defined in Ref. 3, is an integral involving radial wave functions. $N(E_F)$ is the total density of states (DOS) at E_F and N_l are the angular momentum components of the DOS inside the muffin-tin spheres. Equation (1) is exact up to $l=1$, but for higher values of l it involves non-spherical corrections. The necessary input to Eq. (1) was generated from a set of full potential linearized augmented plane-wave (LAPW) calculations that we performed for fcc B using touching muffin-tin (MT) spheres, and the tetrahedron method for the DOS.

We also performed an LAPW calculation for α_{12} B. This is a rhombohedral structure, space group $R\bar{3}m-D_{3d}^5$ (No. 166), with measured lattice parameters⁵ $a=b=c=9.56$ a.u. and angles $\alpha=\beta=\gamma=58.06^\circ$. The energy bands of α_{12} B are shown in Fig. 1. We obtain a valence bandwidth of 15.9 eV and an energy gap of 1.47 eV separating valence and conduction bands. The angular momentum character of the states can be seen from Fig. 2, which shows the expected dominance of the p states through the whole spectrum.

For fcc B we calculated an equilibrium lattice parameter $a=5.37$ a.u. and a bulk modulus of 282 GPa, to be compared with the values of 5.34 a.u. and 269 GPa reported by Mailhot *et al.*² At $a=4.60$ a.u., we find that the pressure is 307 GPa, near the region where superconductivity is observed.¹ There we find a bulk modulus of 976 GPa, with shear moduli $C_{11}-C_{12}=1101$ GPa and $C_{44}=134$ GPa, showing that the fcc structure is at least metastable above this pressure. We note that for $a=4.60$ a.u. the nearest-neighbor B-B distance is 3.25 a.u., which is close to the B-B distance (3.37 a.u.) in the recently discovered superconductor MgB₂. This leads us to speculate that superconductivity may have the same origin in both materials.

The band structure of fcc B confirms a metallic phase for all lattice parameters, with a rapidly increasing bandwidth going to higher pressures. The occupied bandwidth is 1.43 Ry at equilibrium and 1.88 Ry at $a=4.60$ a.u. The energy bands for $a=4.60$ a.u. are shown in Fig. 3. A fairly flat band appears near E_F in the XW direction at all lattice parameters. At X the band has strong s character, becoming p -like at W . This situation is reminiscent of MgB₂, where a similar flat

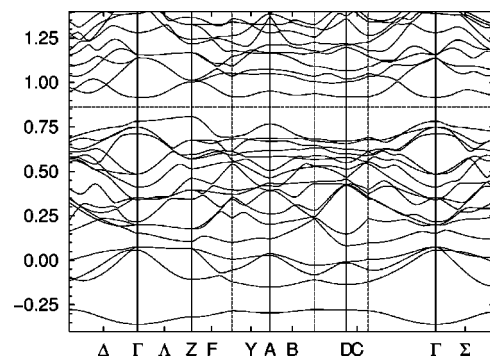


FIG. 1. The electronic band structure of α_{12} B calculated by the LAPW method. The solid vertical lines represent high-symmetry points, while the dashed vertical lines represent zone boundaries. The horizontal line near 0.85 Ry is the Fermi level.

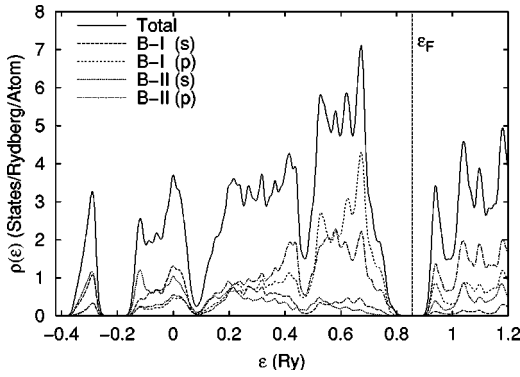


FIG. 2. The electronic density of states of $\alpha_{12}\text{B}$, computed by smearing the eigenvalues of an LAPW calculation using a Fermi temperature of 5 meV. The s and p decomposition is shown for both types of atoms (B I and B II) in the $\alpha_{12}\text{B}$ structure.

band just above E_F has been identified as the origin of superconductivity in this compound.^{6–9} This band appears to be responsible for a peak in the DOS at E_F shown in Fig. 4. We present the corresponding two-dimensional cross section of the Fermi surface in Fig. 5, showing hole pockets near X and electron pockets near W . Also in Fig. 4 we find the s , p , and d distributions of the DOS. In Fig. 4 we confirm that the strongest DOS component is that from the p states. The values of DOS at E_F enter Eq. (1) above for the evaluation of the Hopfield parameter η . The input and results using Eq. (1) at four lattice parameters are listed in Table I.

We note that in Table I the l components of the DOS are given within the MT spheres (as is the case in Fig. 4), and therefore they do not add up to the value of $N(E_F)$. The p component $N_p(E_F)$ is, as expected, dominant and is about 60% of the value of the total inside the MT. The p - d scattering, resulting from the $l=1$ term in Eq. (1), gives by far the largest contribution to the Hopfield parameter η . For the high-pressure case ($a=4.60$ a.u.), $\eta_{pd}=0.79\eta_{tot}$. The value of η_{tot} is approximately the same as the value of $\eta=14.13$ eV/Å² previously reported⁴ for metallic hydrogen at a higher pressure of 467 GPa. It is also interesting to note that the boron value of η at equilibrium is very close to the value $\eta=7.627$ eV/Å² for Nb,¹⁰ a typical transition-metal superconductor, where the d - f scattering is the dominant term in Eq. (1).

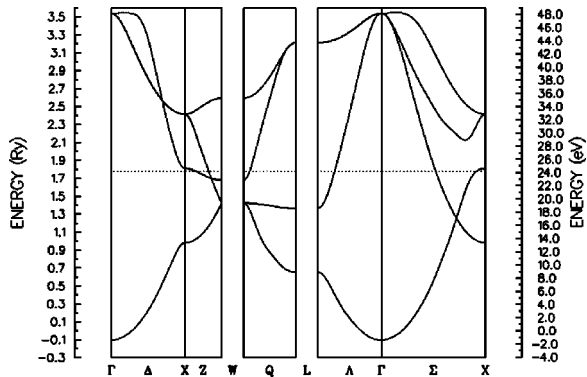


FIG. 3. The electronic band structure of fcc B at the lattice constant 4.60 a.u.

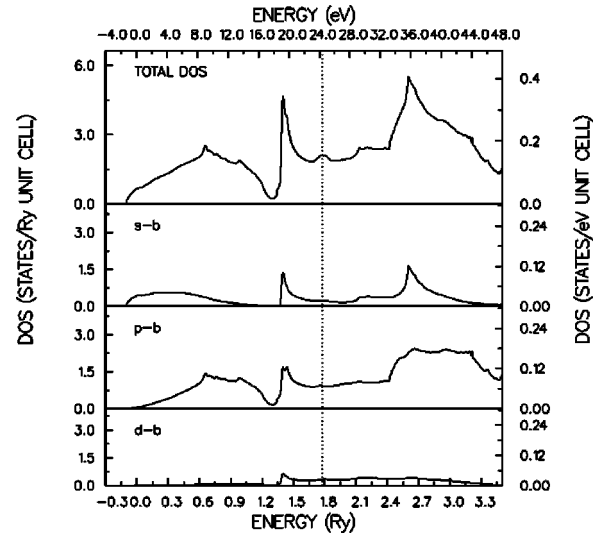


FIG. 4. The electronic density of states of fcc B at the lattice constant 4.60 a.u., as determined by the tetrahedron method.

To evaluate the critical temperature T_c we have used the McMillan¹¹ approach defining an electron-phonon coupling constant $\lambda = \eta/M\langle\omega^2\rangle$. Here η is calculated from Eq. (1) as discussed above. For the average phonon frequency $\langle\omega\rangle$ we followed Eremets *et al.*¹ and chose a range of values from 1200 K to 1400 K. The resulting λ is in the range 0.53 to 0.39, respectively. Continuing we use the McMillan equation

$$T_c = \frac{\langle\omega\rangle}{1.45} \exp\left[-\frac{1.04(1+\lambda)}{\lambda - \mu^*(1+0.62\lambda)}\right]. \quad (2)$$

We solve Eq. (2) for five values of the Coulomb pseudopotential $\mu^*=0.09$ to 0.13, and in the above range of ω and λ values. The corresponding values of T_c are shown in Fig. 6. Within the uncertainty of the values of the frequency ω

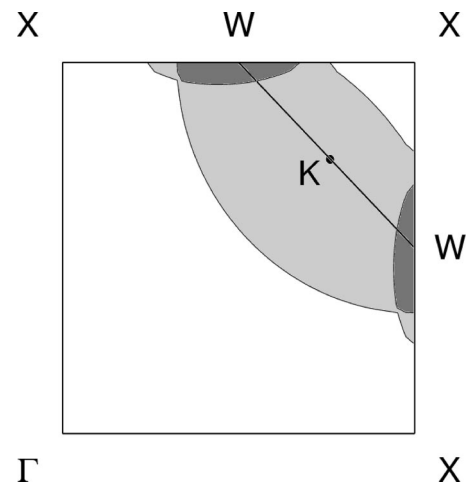


FIG. 5. The Fermi surface in the $\langle 001 \rangle$ plane of fcc Boron at the lattice constant 4.60 a.u. The unshaded areas represent regions where one band is occupied. (Compare with Fig. 3.) In the lightly shaded regions two bands are filled, while the darkest regions contain three occupied bands. The curves between these regions represent the Fermi surface.

TABLE I. Radius of the muffin-tin sphere R_s , Fermi level E_F , total DOS at E_F , angular components of the DOS N_l , free-scatterer DOS $N_l^{(1)}$, scattering phase shifts δ_l , l components of the Hopfield parameter η , and the total value of η . The three columns are headed by the lattice parameters and the corresponding pressures.

a (a.u.)	4.60	5.00	5.37	6.00
P (GPa)	307	89	0	-50
R_s (a.u.)	1.626	1.768	1.898	2.121
E_F (Ry)	1.776	1.408	1.139	0.784
$N(E_F)$ [states/(Ry spin)]	1.050	1.328	1.475	1.514
$N_s(E_F)$ [states/(Ry spin)]	0.114	0.172	0.233	0.276
$N_p(E_F)$ [states/(Ry spin)]	0.469	0.568	0.637	0.769
$N_d(E_F)$ [states/(Ry spin)]	0.164	0.193	0.195	0.155
$N_s^{(1)}$ [states/(Ry spin)]	0.187	0.231	0.270	0.324
$N_p^{(1)}$ [states/(Ry spin)]	0.818	1.058	1.334	1.991
$N_d^{(1)}$ [states/(Ry spin)]	0.010	0.105	0.106	0.099
δ_s	-0.109	0.099	0.298	0.658
δ_p	0.682	0.761	0.835	0.962
δ_d	0.031	0.029	0.027	0.021
η_{sp} (eV/Å ²)	2.945	1.576	0.820	0.150
η_{pd} (eV/Å ²)	11.555	9.172	6.960	4.048
η_{df} (eV/Å ²)	0.089	0.063	0.044	0.022
η_{tot} (eV/Å ²)	14.588	10.811	7.824	4.220

and near the value $\omega = 1250$ K, our model predicts T_c values in the range of the experiment that validates the assertion of an electron-phonon mechanism.

Finally, we want to comment on the pressure dependence of T_c . Our calculations show that the parameter η goes from

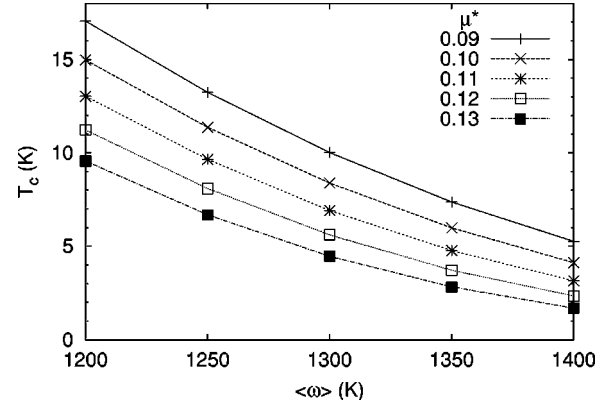


FIG. 6. The superconducting transition temperature T_c of fcc Boron, as determined by the McMillan equation (2), as a function of the RMS phonon frequency $\langle\omega\rangle$ at various values of μ^* .

the value 7.82 eV/\AA^2 at the equilibrium fcc volume to the value of 14.59 eV/\AA^2 at a pressure of 307 GPa. It is important to note that $N(E_F)$ follows the opposite trend, i.e., it reduces with increasing pressure. Assuming that the variation of $\langle\omega\rangle$ with pressure is not as strong as the variation of η , we propose that the rapid increase of η is responsible for the observed increase of T_c with pressure.

In summary, we find that LAPW calculations, the RMT theory, and a McMillan analysis for T_c give a good description of superconductivity in boron at high pressures.

ACKNOWLEDGMENT

This work was supported by the U.S. Office of Naval Research.

*Electronic address: papacon@dave.nrl.navy.mil

†Electronic address: mehl@dave.nrl.navy.mil

¹M. I. Eremets, V. V. Struzhkin, H. Mao, and R. J. Hemley, *Science* **293**, 272 (2001).

²C. Mailhot, J. B. Grant, and A. K. McMahan, *Phys. Rev. B* **42**, 9033 (1990).

³G. D. Gaspari and B. L. Gyorffy, *Phys. Rev. Lett.* **28**, 801 (1972).

⁴D. A. Papaconstantopoulos and B. M. Klein, *Ferroelectrics* **16**, 307 (1977).

⁵*Pearson's Handbook of Crystallographic Data for Intermetallic Phases*, 2nd ed., edited by P. Villars and L. D. Calvert (ASM International, Materials Park, OH, 1991).

⁶J. M. An and W. E. Pickett, *Phys. Rev. Lett.* **86**, 4366 (2001).

⁷J. Kortus, I. I. Mazin, K. D. Belashchenko, V. P. Antropov, and L. L. Boyer, *Phys. Rev. Lett.* **86**, 4656 (2001).

⁸M. J. Mehl, D. A. Papaconstantopoulos, and D. J. Singh, *Phys. Rev. B* **64**, 140509(R) (2001).

⁹Y. Kong, O. V. Dolgov, O. Jepsen, and O. K. Andersen, *Phys. Rev. B* **64**, 020501 (2001).

¹⁰D. A. Papaconstantopoulos, L. L. Boyer, B. M. Klein, A. R. Williams, V. L. Moruzzi, and J. F. Janak, *Phys. Rev. B* **15**, 4221 (1977).

¹¹W. L. McMillan, *Phys. Rev.* **167**, 331 (1968).